

Fluffy dust forms icy planetesimals by static compression

Akimasa Kataoka^{1,2}, Hidekazu Tanaka³, Satoshi Okuzumi⁴, and Koji Wada⁵

¹ Department of Astronomical Science, School of Physical Sciences, Graduate University for Advanced Studies (SOKENDAI), Mitaka, Tokyo 181-8588, Japan

e-mail: akimasa.kataoka@nao.ac.jp

² National Astronomical Observatory of Japan, Mitaka, Tokyo 181-8588, Japan

³ Institute of Low Temperature Science, Hokkaido University, Kita, Sapporo 060-0819, Japan

⁴ Department of Earth and Planetary Sciences, Tokyo Institute of Technology, Meguro, Tokyo, 152-8551, Japan

⁵ Planetary Exploration Research Center, Chiba Institute of Technology, Narashino, Chiba, 275-0016, Japan

January 30, 2019

ABSTRACT

Context. In planetesimal formation theory, several barriers have been proposed, which are bouncing, fragmentation, and radial drift problems. To understand the structure evolution of dust aggregates is a key in the planetesimal formation. Dust grains become fluffy by coagulation in protoplanetary disks. However, once they become fluffy, they are not sufficiently compressed by collisional compression to form compact planetesimals.

Aims. We aim to reveal the pathway of the dust structure evolution from dust grains to compact planetesimals.

Methods. Using the compressive strength formula, we analytically investigate how fluffy dust aggregates are compressed by static compression due to ram pressure of the disk gas and self gravity of the aggregates in protoplanetary disks.

Results. We reveal the pathway of the porosity evolution from dust grains via fluffy aggregates to form planetesimals, circumventing the barriers in planetesimal formation. The aggregates are compressed by the disk gas to the density of 10^{-3}g/cm^3 in coagulation, which is more compact than the case with collisional compression. Then, they are compressed more by self gravity to 10^{-1}g/cm^3 when the radius is 10 km. Although the gas compression decelerate the growth, they grow enough rapidly to avoid the radial drift barrier when the orbital radius is $\lesssim 6$ AU in a typical disk.

Conclusions. We propose fluffy dust growth scenario from grains to planetesimals. It enables the icy planetesimal formation in a wide range beyond the snowline in protoplanetary disks. This result proposes a concrete initial condition of planetesimals for the later stages of the planet formation.

Key words. planets and satellites: formation – methods: analytical – protoplanetary disks

1. Introduction

Planetesimals, the seeds of planets, are believed to form by coagulation of dust grains in protoplanetary disks. How micron-sized dust grains grow to kilometer-sized planetesimals has been an unsolved problem toward the complete planet formation theory; the intermediate-sized bodies have been believed to be poorly sticky (Zsom et al. 2010), easily disrupted by collisions (Blum & Wurm 2008), or to quickly fall onto the central star (Adachi et al. 1976; Weidenschilling 1977).

Several possibilities have been proposed to overcome these barriers (Johansen et al. 2007; Pinilla et al. 2012; Windmark et al. 2012; Lambrechts & Johansen 2012; Ros & Johansen 2013; Garaud et al. 2013). However, there has been no coherent scenario which explains planetesimal formation from dust grains avoiding all of the barriers.

The internal structure evolution is a key to understand the dust coagulation to form planetesimals. Figure 1(a) and (b) show the schematic diagram of the structure evolution previously considered. Dust grains become porous aggregates composed of sub-micron monomer particles by coagulation in protoplanetary disks as illustrated in Fig.1(a) (Smirnov 1990; Meakin 1991; Kempf et al. 1999; Blum & Wurm 2000; Krause & Blum 2004; Paszun & Dominik 2006). When the dust aggregates become massive, they are gradually compacted or disrupted at dust-dust collisions because of the increase in the impact energy as il-

lustrated in Fig.1(b) (Dominik & Tielens 1997; Wada et al. 2007, 2008, 2009; Suyama et al. 2008, 2012; Paszun & Dominik 2008, 2009; Okuzumi et al. 2012).

The growth via fluffy aggregates has been proposed to be one possible scenario to overcome the barriers in Okuzumi et al. (2012). They have shown that fluffy aggregates rapidly coagulate to avoid the radial drift problem. On the other hand, though the aggregates are compressed by dust-dust collisions, their internal density remains $\rho \sim 10^{-5}\text{g/cm}^3$ (Suyama et al. 2008; Okuzumi et al. 2012). This is inconsistent with the fact that planetesimals are believed to have $\rho \sim 0.1\text{g/cm}^3$ as well as comets, the remnants of planetesimals (A'Hearn 2011). Therefore, other mechanisms to compress the fluffy aggregates are required.

In this paper, we introduce static compression of aggregates due to ram pressure of the disk gas and self gravity in protoplanetary disks, as illustrated in Fig.1(c) and (d). We use the compressive strength of porous aggregates numerically derived by Kataoka et al. (2013) to obtain the porosity (equivalent to the internal density) of dust aggregates. We show how much the dust aggregates are compressed by the disk gas and self-gravitational compression in their growth. Moreover, we investigate whether the growth is enough rapid to avoid the radial drift barrier, by comparing the dust growth and radial drift timescale.

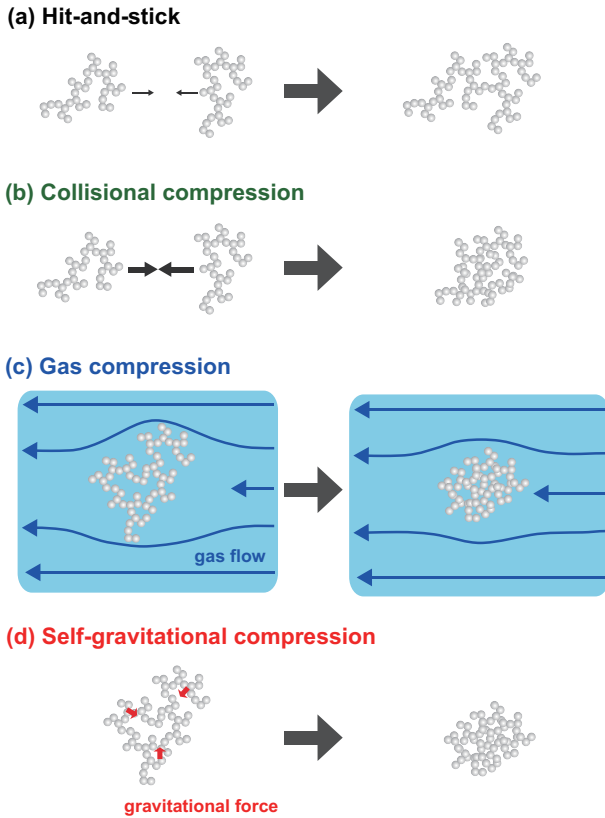


Fig. 1. Schematic drawing to illustrate the dust growth via fluffy aggregates. (a) The dust aggregate hit to another aggregate to be stick. This makes dust density lower, and it occurs in a very early stage of the dust growth. (b) When the collisional speed is enough high to disrupt the dust aggregate, they are compressed. (c) Dust aggregate has a velocity difference against gas, and they feel the ram pressure by the gas. The ram pressure statically compresses the dust aggregate. (d) When the dust aggregate become as massive as they do not support their structure, they are compressed by self gravity of themselves.

2. Method

The compressive strength of a highly porous dust aggregate, P , is given by (Kataoka et al. 2013)

$$P = \frac{E_{\text{roll}}}{r_0^3} \left(\frac{\rho}{\rho_0} \right)^3, \quad (1)$$

where ρ is the mean internal density of the dust aggregate, r_0 the monomer radius, ρ_0 the material density, and E_{roll} the rolling energy, which is the energy for rolling of a particle over a quarter of the circumference of another particle in contact (Dominik & Tielens 1997; Wada et al. 2007). In this paper, we adopt $\rho_0 = 1.0 \text{ g/cm}^3$, $r_0 = 0.1 \mu\text{m}$, and $E_{\text{roll}} = 4.74 \times 10^{-9} \text{ erg}$, which correspond to icy particles. E_{roll} is proportional to the critical displacement, which has an uncertainty from 2 \AA to 30 \AA (Dominik & Tielens 1997; Heim et al. 1999). For later discussion, note that the dust density is proportional to $E_{\text{roll}}^{1/3}$ and thus the uncertainty little affects the resultant dust density.

When a dust aggregate feels a pressure which is higher than its compressive strength, the aggregate is quasi-statically compressed until its strength equals to the pressure. We define the dust internal density where the compressive strength equals a given pressure as a equilibrium density ρ_{eq} . Using Eq.(1), we

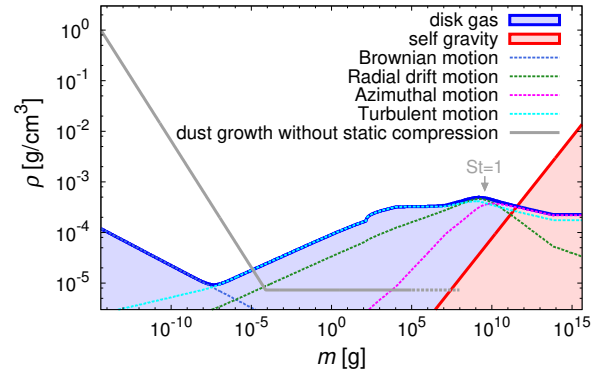


Fig. 2. The equilibrium dust density at 5AU in MMSN disk. The blue thick solid line represents the equilibrium density of gas pressure where the ram pressure of gas is equal to the compressive strength of the dust aggregate. The thin dotted lines represent the component of gas ram pressure, which are induced by the velocity difference between gas and dust, such as Brownian motion, radial drift motion, azimuthal motion, and turbulent motion. The red solid line represents the equilibrium density of self gravity. The blue and red shaded region represent where the compressive strength of the dust aggregate is lower than the pressure of gas or self-gravity, so these aggregates are compressed until their density becomes the equilibrium density. We also plot the dust growth path without static compression (Okuzumi et al. 2012).

obtain ρ_{eq} as

$$\rho_{\text{eq}} = \left(\frac{r_0^3 P}{E_{\text{roll}}} \right)^{1/3} \rho_0. \quad (2)$$

As a source of the pressure, we consider that due to ram pressure of the disk gas or self gravity of the aggregate.

We obtain ram pressure of the disk gas as follows. Here, we consider a dust aggregate of mass m and radius r , and it is moving in the disk gas with velocity v against the gas. The pressure P_{gas} against the aggregate can be defined as the gas drag force divided by the geometrical cross section: $P_{\text{gas}} \equiv F_{\text{drag}}/A$, where $F_{\text{drag}} = mv/t_s$, $A = \pi r^2$, and t_s is the stopping time of the aggregate. While the pressure has both compressive and tensile components, we assume that the pressure is compressive. Thus, we obtain the pressure as

$$P_{\text{gas}} = \frac{mv}{\pi r^2 t_s}. \quad (3)$$

To obtain t_s and v , the typical gas drag law is adopted. The gas drag law is Epstein regime when the dust radius is less than $4/9$ times the mean free path of gas, and Stokes regime on the other hand if Reynolds number is less than unity (see Eq.(4) in Okuzumi et al. (2012) for example). When Reynolds number exceeds unity, the gas drag law changes as a function of Reynolds number (see Eq.(8a) to Eq.(8c) in Weidenschilling (1977)). The drag force is determined by the relative velocity of the gas and dust. The relative velocity is induced by Brownian motion, radial drift, azimuthal drift, and turbulence. We use the closed formula of turbulence model (Ormel & Cuzzi 2007), and assume the turbulent parameter $\alpha_D = 10^{-3}$ except for the strong turbulence case where $\alpha_D = 10^{-2}$.

We assume the minimum mass solar nebula, which was constructed based on our solar system (Hayashi 1981). At a

radial distance R from the central star, the gas surface density profile is $1700 \text{ g/cm}^2 \times (R/1\text{AU})^{-1.5}$, and the dust-to-gas mass ratio is 0.01. The temperature profile adopted is $137 \text{ K} \times (R/1\text{AU})^{-3/7}$, which corresponds to midplane temperature (Chiang et al. 2001). This is cooler than optically thin disk models to focus on the dust coagulation in the midplane.

We also calculate the self-gravitational pressure as follows. Although the gravitational pressure has distribution in the aggregates, we simply assume the uniform pressure inside the aggregates. We define the force on the dust aggregates as $F = Gm^2/r^2$, and the area $A = \pi r^2$. Thus, the self-gravitational pressure is

$$P_{\text{grav}} = \frac{Gm^2}{\pi r^4}. \quad (4)$$

Note that the equilibrium density of self-gravitational compression does depend only on dust mass and internal density not on the disk properties.

3. Results

First, we calculate the equilibrium density of dust aggregates in a wide range in mass, where their compressive strength is equal to the gas or self-gravitational pressure. Figure 2 shows the equilibrium dust density against dust mass at 5 AU in the disk. If the gas or self-gravitational pressure is higher than the compressive strength, the dust aggregate is compressed to achieve the equilibrium density because the strength is higher in denser dust aggregates. In other words, the equilibrium density represents a lower limit of the dust density in the disk. We also plot the collisional growth path without static compression (Okuzumi et al. 2012); the dust aggregates initially grow with fractal dimension of 2, and then, when the impact energy of dust-dust collisions reaches the rolling energy, the internal density becomes almost constant. The evolutionary track should trace the higher density of the growth with collisional compression and the equilibrium density of static compression. Therefore, we conclude that dust growth is initially fractal, and then the gas compression becomes effective before collisional compression occurs at 5 AU in the disk.

Figure 3 shows the pathways of the dust growth in mass-density space at 5 and 8 AU from the central star. Here, we assume that the dust aggregates have no mass or volume distribution. The first growth mode is hit-and-stick, where the fractal dimension is 2. As dust aggregates become massive, the gas compression becomes effective. Once the gas compression occurs, the equilibrium density is higher in more massive aggregates until the Stokes number, that is the stopping time normalized by the orbital timescale, becomes unity, so the aggregates always keep the equilibrium density in coagulation. The gas compression keeps effective until the dust aggregates grow so massive that self-gravitational compression is more effective than the gas compression. The self-gravitational compression becomes effective when the mass becomes $\sim 10^{11}$ g. Once the gravitational compression becomes effective, the density increases with the mass of the power of 5/2, although the gas compression makes the dust density almost constant because of the constant velocity difference of the gas and dust of the head wind in azimuthal direction. Therefore, the final stage is determined by the self-gravitational compression. We find that the dust aggregates should be compressed to have their density 0.1 g/cm^3 when their mass is $\sim 10^{18}$ g.

The density and mass of the final product is close to comets, which are considered to be the remnants of planetesimals. We

also plot the properties of several comets which are well known in the density and mass in Fig. 3 (A'Hearn 2011). The comets have their mass of $\sim 10^{16}$ g and their internal mass density of $\sim 0.1 \text{ g/cm}^3$. There is a two orders-of-magnitude discrepancy in mass between the final product of our calculation and the comets. The mass of comets would be finally determined by collisional fragmentation or melting of planetesimals.

We estimate the dust growth timescale by coagulation and the radial drift timescale. Assuming that aggregates have no mass or volume distribution, the growth time is defined as $m/\rho_d \pi r^2 \Delta v$, where ρ_d is the spatial mass density of dust aggregates and Δv is the velocity difference between the dust aggregates, which is assumed to be the root mean square of Brownian motion and turbulent motion (see Eq. (32) in Okuzumi et al. (2012)). For the velocity induced by turbulence, we use velocity difference of dust and gas as dust-dust velocity for simplicity. We include the dust sedimentation by considering the dust scale-height (Brauer et al. 2008). The drift timescale is defined as the orbital radius divided by the radial drift velocity. We define the dust aggregates where the drift timescale is less than 30 times the growth timescale drift to the central star (Okuzumi et al. 2012).

We show that the revealed pathway still overcomes the radial drift problem. Figure 3 also illustrates the region where the dust aggregates radially drift inward before they grow. Even when the dust aggregates become massive and their Stokes number is unity, the dust growth time is still shorter than the drift at 5 AU. In outer radius of the disk, for example at 8 AU, the dust aggregates drift inward before growth (top right of Fig. 3). However, if the disk is two times as massive as MMSN, the dust aggregates successfully break the radial drift problem (bottom right of Fig. 3). Therefore, the fluffy dust can grow to planetesimals more inside in protoplanetary disks.

Fluffy dust also breaks through the bouncing barrier. Solid bodies have been shown to bounce in some situations (Güttler et al. 2010). However, both numerical simulations and experiments have shown that highly porous aggregates do not bounce when $\phi \lesssim 0.15$ (Langkowski et al. 2008; Wada et al. 2011; Seizinger & Kley 2013; Kothe et al. 2013). Thus, the bouncing is not a strong difficulty for the growth of highly porous aggregates.

The fragmentation barrier is not a serious problem when considering icy particles. The dust aggregates are not significantly fragmented and grow through collisions as long as their collision velocity is $< 60 \text{ m/s}$ (Wada et al. 2009). The collisional velocity becomes maximum when the Stokes number is unity. It is the square root of α_D times the sound speed of gas. In case of $\alpha_D = 10^{-3}$, the maximum velocity is $\sim 17 \text{ m/s}$ at 5AU, so the dust aggregates can avoid significant disruption. In case of $\alpha_D = 10^{-2}$, on the other hand, the velocity reaches $\sim 54 \text{ m/s}$, comparable to the critical velocity. Thus, we should carefully discuss the fragmentation in strong turbulent disks. Note that the turbulent velocity is lower than the original MMSN model, where the temperature is determined by balance between the stellar radiation and the reemission for each position. This is because we focus on the midplane where the temperature is lower, and thus the velocity is also lower than the irradiated surface.

However, when considering silicate particles, it is difficult to break through the fragmentation barrier. Inside the snowline, the ice is sublimated and the dominant material is silicate particles. The critical velocity of fragmentation of silicate is $\sim 6 \text{ m/s}$ (Wada et al. 2009). Thus, the silicate planetesimal formation is still an open question.

In the final stage of the coagulation, the runaway growth begins. We estimate the dust mass where the dust-dust collision ve-

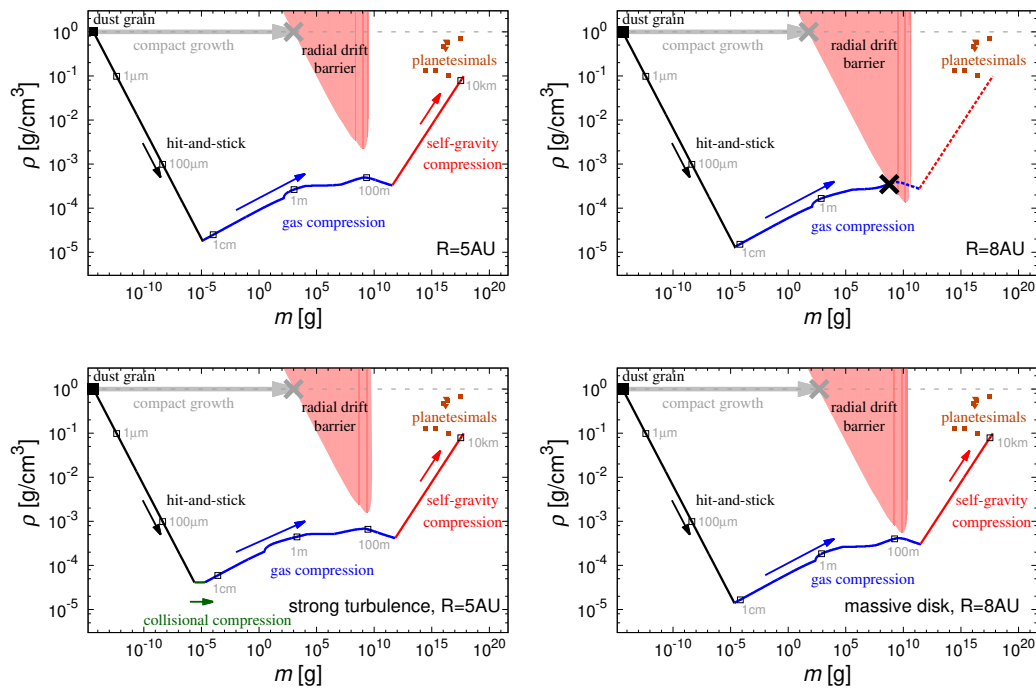


Fig. 3. The pathways in the planetesimal formation in the minimum mass solar nebula model. The gray line shows the constant density evolutionary track, which corresponds to the compact growth. The black, green, blue, and red lines are the evolutionary track through dust coagulation via fluffy aggregates. Each line represents different mechanisms of dust coagulation, which are hit-and-stick, collisional compression, gas compression, and self-gravity compression. The red shaded region represents where the radial drift timescale is less than the growth timescale, which is equivalent to radial-drift region. The brown squares indicates the properties of comets, and the triangles represent their upper limit. The radii of dust aggregates for $1 \mu\text{m}$, 1cm , 1m , 100m , and 10km are also written. (Top left): for 5 AU in orbital radius. (Top right): for 8 AU in orbital radius. The cross point represents where the dust fall onto the central star. (Bottom left): for 5 AU in strong turbulence model where $\alpha_D = 10^{-2}$. (Bottom right): for 8 AU in two times as massive as MMSN model.

locity induced by turbulence exceeds the escape velocity of the dust. When the dust becomes as massive as $\sim 10^{15} \text{g}$, the runaway growth starts. The dust internal density is still as small as $\sim 10^{-2}$, this means that geometrical cross section is larger than the compact case. This will make the runaway growth faster but the whole scenario does not change as shown in the N -body simulations (Kokubo & Ida 1996).

In conclusion, we revealed the pathway of the porosity evolution of dust aggregates to form planetesimals by introducing static compression. We also showed that icy dust growth on the pathway avoid the bouncing, fragmentation, and radial drift barriers. This scenario can provide a planetesimal distribution as a concrete initial condition of the later stages of the planet formation.

Acknowledgements. A.K. is supported by the Research Fellowship from JSPS for Young Scientists (24-2120).

References

Adachi, I., Hayashi, C., & Nakazawa, K. 1976, *Progress of Theoretical Physics*, 56, 1756
A’Hearn, M. F. 2011, *ARA&A*, 49, 281
Blum, J. & Wurm, G. 2000, *Icarus*, 143, 138
Blum, J. & Wurm, G. 2008, *ARA&A*, 46, 21
Brauer, F., Dullemond, C. P., & Henning, T. 2008, *A&A*, 480, 859
Chiang, E. I., Joungh, M. K., Creech-Eakman, M. J., et al. 2001, *ApJ*, 547, 1077
Dominik, C. & Tielens, A. G. G. M. 1997, *ApJ*, 480, 647

Garaud, P., Meru, F., Galvagni, M., & Olczak, C. 2013, *ApJ*, 764, 146
Güttler, C., Blum, J., Zsom, A., Ormel, C. W., & Dullemond, C. P. 2010, *A&A*, 513, A56
Hayashi, C. 1981, *Progress of Theoretical Physics Supplement*, 70, 35
Heim, L.-O., Blum, J., Preuss, M., & Butt, H.-J. 1999, *Physical Review Letters*, 83, 3328
Johansen, A., Oishi, J. S., Mac Low, M.-M., et al. 2007, *Nature*, 448, 1022
Kataoka, A., Tanaka, H., Okuzumi, S., & Wada, K. 2013, *A&A*, 554, A4
Kempf, S., Pfalzner, S., & Henning, T. K. 1999, *Icarus*, 141, 388
Kokubo, E. & Ida, S. 1996, *Icarus*, 123, 180
Kothe, S., Blum, J., Weidling, R., & Güttler, C. 2013, *Icarus*, 225, 75
Krause, M. & Blum, J. 2004, *Physical Review Letters*, 93, 021103
Lambrechts, M. & Johansen, A. 2012, *A&A*, 544, A32
Langkowski, D., Teiser, J., & Blum, J. 2008, *ApJ*, 675, 764
Meakin, P. 1991, *Reviews of Geophysics*, 29, 317
Okuzumi, S., Tanaka, H., Kobayashi, H., & Wada, K. 2012, *ApJ*, 752, 106
Ormel, C. W. & Cuzzi, J. N. 2007, *A&A*, 466, 413
Paszun, D. & Dominik, C. 2006, *Icarus*, 182, 274
Paszun, D. & Dominik, C. 2008, *A&A*, 484, 859
Paszun, D. & Dominik, C. 2009, *A&A*, 507, 1023
Pinilla, P., Birnstiel, T., Ricci, L., et al. 2012, *A&A*, 538, A114
Ros, K. & Johansen, A. 2013, *A&A*, 552, A137
Seizinger, A. & Kley, W. 2013, *A&A*, 551, A65
Smirnov, B. M. 1990, *Phys. Rep.*, 188, 1
Suyama, T., Wada, K., & Tanaka, H. 2008, *ApJ*, 684, 1310
Suyama, T., Wada, K., Tanaka, H., & Okuzumi, S. 2012, *ApJ*, 753, 115
Wada, K., Tanaka, H., Suyama, T., Kimura, H., & Yamamoto, T. 2007, *ApJ*, 661, 320
Wada, K., Tanaka, H., Suyama, T., Kimura, H., & Yamamoto, T. 2008, *ApJ*, 677, 1296
Wada, K., Tanaka, H., Suyama, T., Kimura, H., & Yamamoto, T. 2009, *ApJ*, 702, 1490
Wada, K., Tanaka, H., Suyama, T., Kimura, H., & Yamamoto, T. 2011, *ApJ*, 737, 36
Weidenschilling, S. J. 1977, *MNRAS*, 180, 57
Windmark, F., Birnstiel, T., Güttler, C., et al. 2012, *A&A*, 540, A73
Zsom, A., Ormel, C. W., Güttler, C., Blum, J., & Dullemond, C. P. 2010, *A&A*, 513, A57